ACADEMIC PRESS

Available online at www.sciencedirect.com

SCIENCE DIRECT®

Journal of Sound and Vibration 262 (2003) 577–589

JOURNAL OF SOUND AND VIBRATION

www.elsevier.com/locate/jsvi

Active control of cylindrical shell with magnetostrictive layer

J.S. Kumar, N. Ganesan, S. Swarnamani, Chandramouli Padmanabhan*

Machine Dynamics Laboratory, Department of Applied Mechanics, Indian Institute of Technology Madras, Chennai 600 036, India

Received 20 November 2001; accepted 28 October 2002

Abstract

This paper analyses the damping characteristics of a titanium shell with a magnetostrictive layer bonded to it. The magnetostrictive layer produces an actuating force required to control vibration in the shell, based on a negative velocity feedback control law. The control input is the current to the solenoid surrounding the shell. In the present study, a finite element formulation, physically consistent with the problem has been developed. Vibration reduction in the shell by changing the position of the magnetostrictive layer and its current carrying actuating coil pair along the shell is investigated.

1. Introduction

Vibration control of structures using smart materials has received considerable attention. Shape memory alloys, piezoelectric ceramics; electro-rheological fluids have been used as smart materials for sensors and/or actuators. Piezoelectric materials have been extensively investigated for use in active vibration and noise control. Of late, magnetostrictive materials are being considered as promising candidates for both sensors and actuators. With the availability of magnetostrictive material Terfenol-D, in various forms including powders, magnetostrictive materials are emerging as a highly attractive material for smart structure applications.

Studies have been reported on electromagnetic-mechanical coupling problems right from the seventies. For instance, Wallerstein and Peach [1] have studied magnetoelastic buckling of beams and plates of magnetically soft materials. Miya et al. [2] reported their experiments and theoretical studies on magnetoelastic buckling of ferromagnetic structures. They have also developed a finite element formulation for this magnetoelastic buckling [3]. Ambartsumian [4] has presented a review of magneto-elasticity in thin plates and shells. Sablik et al. [5] formulated the coupled

*Corresponding author. Tel.: +91-44-2257-8192; fax: +91-44-2257-0509.
E-mail address: mouli@iitm.ac.in (C. Padmanabhan).

0022-460X/03/$ - see front matter
doi:10.1016/S0022-460X(03)00112-3

magneto-elastic theory for magnetostrictive hysteresis. Hudson et al. [6] have investigated elastic and magnetomechanical coupling models for polymer-bonded Terfenol composites. Dapino et al. [7] have made a significant contribution to the modelling of the structural-magnetic strain developed in a magnetostrictive transducer. They have calculated and validated the strains developed by considering both the rotation of the moments within the material in response to the applied field and the elastic property of the material. Yamamoto et al. [8] have developed and analyzed the application of a three-dimensional magnetostrictive sensor. Krishnamurthy et al. [9] and Reddy and Barbosa [10] have studied the use of magnetostrictive material for vibration control of flexible beams. They have considered the magnetostrictive material to be one full layer in the laminate, with partly covered actuating coils. The actuating coils were modelled as solenoids, with the current input to the solenoid being considered as a function of space and time. Though it is mathematically possible to model the current in the solenoid in this manner, it is not physically reasonable to provide a spatially varying current throughout the length of the coil. The magnetic field induced by the solenoid is more or less constant within the solenoid length, but reduces to an insignificant amount, within a short axial distance after the end of the solenoid. This residual magnetic field will stimulate the magnetostrictive layer, an effect not considered in their investigations.

It is also found from the literature that there is no reported investigation, which deals with vibration control of shells with a magnetostrictive layer. Shell vibration attenuation in gun or cannon barrels and in cylindrical pipes conveying fluids using magnetostrictive materials is a potential application area. Hence in the present paper an attempt is made to control vibrations in cylindrical shell using a magnetostrictive layer. The shell under study is discretized into finite elements and the magnetostrictive layer of the size of a single element along with its actuating coil is located at various positions to demonstrate the effective damping characteristics. Magnetostrictive layer, Terfenol-D, is an alloy or terbium, iron and dysprosium. The magnetostrictive layer responds to the magnetic and mechanical stimuli. The magnetostrictive layer expands when excited with a magnetic field allowing it to be used as embedded actuators. On the other hand when the layer is mechanically strained, it generates an induced voltage across a sensing coil placed near the vincity. The magnetomechanical coefficient depends upon the pre-stress and magnetic field. For the purpose of illustration, in this work, this layer is assumed to have perfect orientation.

2. Formulation

A typical conventional titanium shell having a small Terfenol-D layer on the top, with a current carrying coil, enclosing them, as shown in Fig. 1, is considered. The magnetostrictive layer is of non-linear nature at moderate or high magnetic drive levels. To model the magnetostrictive layer with a linear constitutive relation, the necessary low magnetic field regimes is obtained by applying a biasing current to the surrounding coils. The low magnetic field intensity induces an actuation stress in the Terfenol-D layer. The width of the coil is made as small as possible to achieve the required variation of control forces in this region.

Consider a cylindrical four-nodded shell element with seven-degree-of-freedom at each node as shown in Fig. 2. The shell element is developed based on the shell element of Zienkiewicz [11].

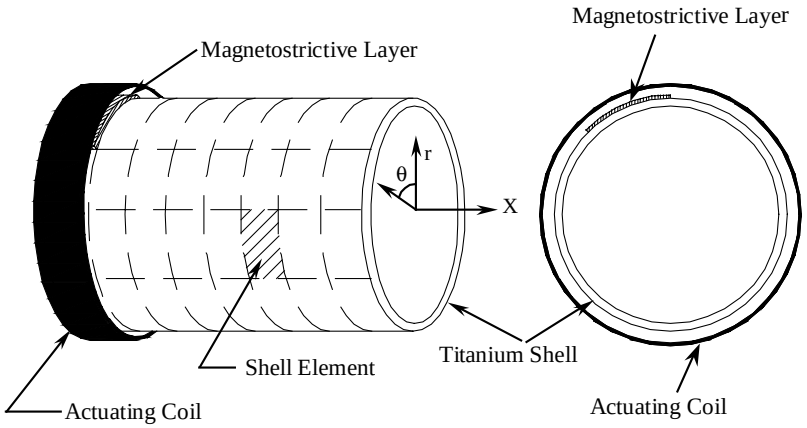

Fig. 1. Conventional titanium shell with magnetostrictive layer.

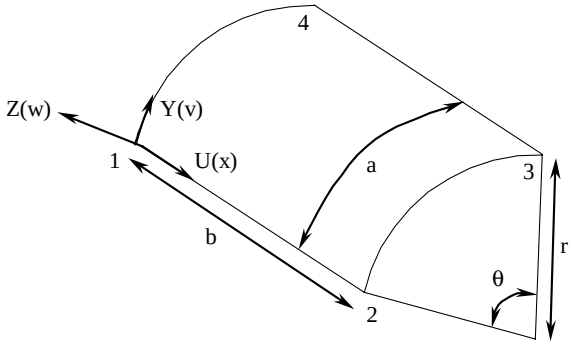

Fig. 2. Conventional cylindrical shell element.

The nodal displacement for a node is expressed as

$$\{\delta\} = \{u, v, (\partial u/\partial\theta), (\partial v/\partial\theta), w, (\partial w/\partial x), (\partial w/\partial\theta)\}^{\mathrm{T}} \tag{1}$$

The deformation in the shell is expressed in terms of the middle surface deformations, u, v and w, which are the meridional, tangential and normal displacements, respectively.

These displacements are now expressed in terms of x and θ, the meridional and circumferential co-ordinate, respectively, as

$$\begin{aligned} w(x,\theta) &= a_1 + a_2x + a_3\theta + a_4x\theta + a_5x^2 + a_6\theta^2 \\ &\quad + a_7x^2\theta + a_8x\theta^2 + a_9x^3 + a_{10}\theta^3 + a_{11}x^3\theta + a_{12}x\theta^3, \\ u(x,\theta) &= a_{13} + a_{14}x + a_{15}\theta + a_{16}x\theta + a_{17}\theta^2 + a_{18}x\theta^2 + a_{19}\theta^3 + a_{20}x\theta^3, \\ v(x,\theta) &= a_{21} + a_{22}x + a_{23}\theta + a_{24}x\theta + a_{25}\theta^2 + a_{26}x\theta^2 + a_{27}\theta^3 + a_{28}x\theta^3, \end{aligned} \tag{2}$$

which can be expressed in matrix form as

$$\{\delta\} = [N]\{A\}, \tag{3}$$

where $\{\delta\}$ is the displacement vector, $[N]$ is the matrix of shape functions and $\{A\}$ is the vector of generalized displacements. The 28 generalized displacements can be now written in terms of nodal displacements as

$$\{\rho\}^{\mathrm{T}} = \begin{bmatrix} u_1, v_1, (\partial u/\partial\theta)_1, (\partial v/\partial\theta)_1, w_1, (\partial w/\partial x)_1, (\partial w/\partial\theta)_1, \\ u_2, v_2, (\partial u/\partial\theta)_2, (\partial v/\partial\theta)_2, w_2, (\partial w/\partial x)_2, (\partial w/\partial\theta)_2, \\ u_3, v_3, (\partial u/\partial\theta)_3, (\partial v/\partial\theta)_3, w_3, (\partial w/\partial x)_3, (\partial w/\partial\theta)_3, \\ u_4, v_4, (\partial u/\partial\theta)_4, (\partial v/\partial\theta)_4, w_4, (\partial w/\partial x)_4, (\partial w/\partial\theta)_4 \end{bmatrix}, \tag{4}$$

where

$$\{\rho\} = [T]\{A\} \quad \text{or} \quad \{A\} = \{T\}^{-1}\{\rho\}. \tag{5}$$

Substituting in Eq. (1) one obtains

$$\{\delta\} = [N][T]^{-1}\{\rho\}. \tag{6}$$

The strain matrix is

$$\{\varepsilon\} = \begin{Bmatrix} \varepsilon_x \\ \varepsilon_\theta \\ \gamma_{x\theta} \\ X_x \\ X_\theta \\ X_{x\theta} \end{Bmatrix} = \begin{Bmatrix} \dfrac{\mathrm{d}u}{\mathrm{d}x} \\ \dfrac{1}{r}\dfrac{\mathrm{d}v}{\mathrm{d}\theta} + \dfrac{w}{r} \\ \dfrac{1}{r}\dfrac{\mathrm{d}u}{\mathrm{d}\theta} + \dfrac{\mathrm{d}v}{\mathrm{d}x} \\ -\dfrac{\mathrm{d}^2 w}{\mathrm{d}x^2} \\ -\dfrac{1}{r^2}\dfrac{\mathrm{d}^2 w}{\mathrm{d}\theta^2} + \dfrac{1}{r^2}\dfrac{\mathrm{d}v}{\mathrm{d}\theta} \\ 2\left(-\dfrac{1}{r}\dfrac{\mathrm{d}^2 w}{\mathrm{d}x\mathrm{d}\theta} + \dfrac{1}{r}\dfrac{\mathrm{d}v}{\mathrm{d}x}\right) \end{Bmatrix}, \tag{7}$$

where $\{\varepsilon\}$ is the strain matrix. The strain can be represented in terms of nodal displacements $\{\rho\}$ as

$$\{\varepsilon\} = [B]\{\rho\}, \tag{8}$$

where $[B]$ is the strain displacement matrix.

The stress–strain relation is given by

$$[\sigma] = [D]\{\varepsilon\}, \tag{9}$$

where $[\sigma]$ is the stress matrix and $[D]$ is the material property matrix which is defined as

$$[D] = \begin{bmatrix} \frac{Eh}{1-v^2} & \frac{vEh}{1-v^2} & 0 & 0 & 0 & 0 \\ & \frac{Eh}{1-v^2} & 0 & 0 & 0 & 0 \\ & & \frac{(1-v)Eh}{2(1-v^2)} & 0 & 0 & 0 \\ & & & \frac{Eh^3}{12(1-v^2)} & \frac{vEh^3}{12(1-v^2)} & 0 \\ & sym & & & \frac{Eh^3}{12(1-v^2)} & 0 \\ & & & & & \frac{(1-v)Eh^3}{24(1-v^2)} \end{bmatrix}, \tag{10}$$

where E is Young's modulus of the titanium shell, h is the width of the shell and v is the poisson ratio. The stiffness and mass matrices of size 28×28 are derived using conventional finite element procedures. They are given as

$$[K] = \int [N]^{\mathrm{T}}[B]^{\mathrm{T}}[D][B][N]r \, \mathrm{d}x \, \mathrm{d}\theta,$$
$$[M] = \int [N]^{\mathrm{T}}[T]^{\mathrm{T}}[T][N]r \, \mathrm{d}x \, \mathrm{d}\theta. \tag{11}$$

The linear constitutive relation for the magnetostrictive layer can be expressed as [9]

$$\varepsilon_x = S\sigma + d_m H, \tag{12}$$

where σ is the stress, ε_x is strain field, S is the compliance of the magnetostrictive layer, d_m is the magnetomechanical-coupling coefficient, and H is the magnetic field intensity. The actuation stress induced in the shell is given by

$$\sigma_a = -E_m d_m H, \tag{13}$$

where E_m is the modulus of elasticity of the magnetostrictive layer. For a coil with n turns, the generated magnetic field is modelled as

$$H(x,t) = nI(t)\varphi(x). \tag{14}$$

In Refs. [7,8], the current is assumed to be a function of space and time, i.e. $I \equiv I(x,t)$ which is physically not possible. For a standard solenoid-type wound coil [12] having a coil radius of r, the coil constant $\varphi(x)$ is given as

$$\varphi(x) = \frac{r^2}{2(r^2+x^2)^{3/2}}. \tag{15}$$

Considering the closed-loop negative velocity proportional feedback control, the current in the coil is proportional to the velocity of the shell. It is assumed that the vibration is sensed using an accelerometer placed at desired locations and the velocity obtained by integration of the signal. The desired locations are those where the magnetostrictive layer and current coil pair are located.

The feedback current to the solenoid is then given as

$$I(t) = -\mathbf{G}\dot{w}_{avg}(t), \tag{16}$$

where $\mathbf{G}$ is the control gain and $\dot{w}_{avg}(t)$ is the average velocity over the element in the finite element model. Rewriting Eq. (14), one obtains

$$H(x,t) = -n\mathbf{G}\dot{w}_{avg}(t)\varphi(x). \tag{17}$$

The moment induced by the actuation stress about the meridional plane is given by

$$M_{11}^{a} = -\left(\frac{z_2^2 - z_1^2}{2}\right) E_m d_m H. \tag{18}$$

Substituting for the field intensity H in the above equation, the expression for moment induced becomes

$$M_{11}^{a} = \left(\frac{z_2^2 - z_1^2}{2}\right) E_m d_m n\mathbf{G}\dot{w}_{avg}\ \varphi(x). \tag{19}$$

The average velocity across an element for the finite element formulation is chosen as

$$\dot{w}_{avg} = \mathbf{G}\dot{w} = \left\langle 0\ 0\ 0\ 0\ \tfrac{1}{4}\ 0\ 0\ 0\ 0\ 0\ 0\ \tfrac{1}{4}\ 0\ 0\ 0\ 0\ 0\ 0\ \tfrac{1}{4}\ 0\ 0\ 0\ 0\ 0\ 0\ \tfrac{1}{4}\ 0\ 0 \right\rangle \frac{\partial w}{\partial t}. \tag{20}$$

The equation for the dynamics of the shell under consideration with the moment actuation becomes

$$[M]\left\{\ddot{x}\right\} + [K]\{x\} - b\left\{\frac{\partial^2 (M_{11}^{a})}{\partial x^2}\right\} = 0. \tag{21}$$

We now assume the variation of the magnetic field within the solenoid to be a constant, i.e. φ is a constant. This leads to a delta function in the last term in Eq. (21).

The last term yields the damping term that is given below

$$-\omega b E_m \mathrm{d} n\mathbf{G}\left(\frac{z_2^2 - z_1^2}{2}\right)\mathbf{V}\{\delta_i\}^{\mathrm{T}} \int \left[\frac{\partial N_i}{\partial x}\right]^{\mathrm{T}} \begin{bmatrix} -\left.\dfrac{\partial w}{\partial x}\right|_{x=0,y=0} + \left.\dfrac{\partial w}{\partial x}\right|_{x=a,y=0} \\ -\left.\dfrac{\partial w}{\partial x}\right|_{x=0,y=b} + \left.\dfrac{\partial w}{\partial x}\right|_{x=a,y=b} \end{bmatrix} \mathrm{d}x\{\delta_i\}. \tag{22}$$

The state-space problem is solved for damping ratio and damped natural frequencies using a standard LAPACK routine DGEGV [13].

3. Validation of magnetostrictive model

It is found from the literature that there is no work which deals with active control of shell with magnetostrictive layer. Hence an attempt is made to compare the finite element results with beam model formulation available in the literature. Krishnamurthy et al. [9] and Reddy and Barbosa [10] have studied the use of magnetostrictive material for vibration control of flexible composite beams. In their formulation, they made an assumption of the feedback current as a function of space and time, which is not physically consistent. If a typical finite element formulation for the

Table 1
Comparison of damping and frequency parameters for the first five modes for a CFRP beam with a simply supported boundary condition

$-\alpha$, ω_d (rad/s) Lay up $(\pm 45/m/0/90)s$				
Mode	Present formulation	Krishnamurthy et al. [9]	Reddy et al. [10]	EBT [10]
1	3.29, 104.85	3.29, 104.88	3.30, 104.82	3.30, 104.85
2	13.19, 419.46	13.19, 419.50	13.16, 418.80	13.20, 419.37
3	29.67, 944.12	29.70, 943.88	29.28, 940.52	29.68, 943.40
4	52.69, 1679.84	52.86, 1678.83	52.10, 1667.68	52.73, 1676.72
5	82.12, 2628.78	82.59, 2621.87	80.80, 2597.09	82.34, 2619.02

Table 2
Comparison of damping and frequency parameters for the first mode for different lay-up sequences of a CFRP beam with simply supported boundary condition

$-\alpha$, ω_d (rad/s) Mode 1				
Lay up	Present formulation	Krishnamurty et al. [9]	Reddy et al. [10]	EBT [10]
$(45/m/-45/0/90)s$	4.61, 102.14	4.60, 102.17	4.62, 102.11	4.62, 102.15
$(m/\pm 45/0/90)s$	5.92, 98.42	5.90, 98.44	5.93, 98.38	5.94, 98.42
$(m/90_4)s$	5.91, 64.65	5.90, 64.65	5.94, 64.64	5.94, 64.65
$(m/0_4)s$	5.93, 143.57	5.90, 143.58	5.94, 143.44	5.94, 143.57

composite beam is derived based *on their assumption*, the damping induced on the beam will be given by the equation

$$\omega b E_m \mathrm{d}n\mathbf{G}\left(\frac{z_2^2 - z_1^2}{2}\right)\left\{\{\delta_a\}\int_0^L\left[\frac{\partial N_a}{\partial x}\right][N_b]\mathrm{d}x\{\delta_b\} + \{\delta_b\}^{\mathrm{T}}\int_0^L\left[\frac{\partial N_b}{\partial x}\right]^{\mathrm{T}}\left[\frac{\partial N_b}{\partial x}\right]\mathrm{d}x\{\delta_b\}\right\}. \quad (23)$$

The first term gives the coupling between axial and bending damping matrices, while the next term gives the uncoupled bending damping matrix. This formulation is used to check the damping parameter α, and damped frequency ω_d, with the results of Reddy and Barbosa [10]. The cross-sectional and inertial coefficients for different lay-ups and materials are taken from the tables in Ref. [10]. The results from the finite element procedure are compared with those of Reddy and Barbosa [10] as shown in Tables 1 and 2.

Table 1 shows the comparison of damping and frequency parameters for the first five modes for a carbon fiber-reinforced plastics (CFRP) beam with a simply supported boundary condition. The lay-up sequence of $[\pm 45/m/0/90]$ is symmetric about the mid-plane of the laminate. The "± 45" denotes one layer with a fiber angle of $+45^\circ$ and the next layer with fiber angle of -45°. The "/" is used to separate the adjacent layer with the different fiber angles. The "m" represents a single layer of magnetostrictive material. The next number "0" represents the fiber angle of 0° and so on. The table shows a good comparison between the present formulation and those obtained by

Reddy and Barbosa with higher order shear deformation theory [10], Euler beam theory (EBT) with first order shear deformation theory [10] and Krishnamurthy et al. [9].

Table 2 shows the influence of the location of the magnetostrictive layer in the z direction and the influence of lamination scheme on the damping and frequency parameters. Results are tabulated for simply supported boundary condition, with four different lay-up schemes. The parameters are compared for the first mode of vibration and it can be seen that the values match very closely.

From these comparisons it is clear that the finite element formulation and solution procedure are consistent and valid.

4. Numerical results and discussions

Now a cylindrical titanium shell of dimension 0.292 m radius and 3.3528 m length with a thickness of 3 mm is considered. On the top of the shell a layer of Terfenol-D material of thickness 1 mm is placed. The properties of the magnetostrictive material, are $E_m = 26.5$ GPa, $\rho_m = 9250$ kg/m^3 and $d = 1.67 \times 10^{-8}$ m/A. The effective radius of the coils, r_c, enclosing the plate is taken to be 0.8 m, with a coil density, n_0 turns/m. The coils are of 38 AWG Copper wires with a density of 8844 kg/m^3. The mass of the coil per unit length assuming $n_0 = 10^4$ is 3.15 kg.

The shell is discretized into an 8×8 mesh, which is 8 elements in the longitudinal direction and 8 elements in radial direction. The length of the actuating coil is also dictated by the size of the element due to finite element discretization. It is assumed that the magnetostrictive material is bonded to the titanium shell on top. The size of the magnetostrictive is equal to one individual finite element on the plate. A detailed parameter study for clamped–clamped boundary conditions has been carried out to examine the effect of coil and magnetostrictive material pair location on damping with a feedback gain of hundred.

The magnetostrictive layer is located at different elements along the radial direction as well as longitudinal direction. The variation of damping ratio with respect to the location of magnetostrictive layer in both the circumferential and radial directions is shown in Figs. 3–10.

Fig. 3 shows the variation of damping ratio when the layer position is shifted along the longitudinal direction. It can be seen from the figure that the pattern is symmetric about the middle of the shell. Modes 1 and 2 show that the damping ratio increases from a minimum near the clamped edge and starts increasing, but when the layer is located near the center of the shell it drops to a minimum value. Mode 3 shows an increase from a lower value as the layer is shifted from the clamped end to the middle but it falls and again increases to a maximum value near the middle of the shell. Modes 4 and 5 have a relatively low damping value through out, while mode 6 depicts a pattern shown by mode 3 but of lower damping value.

Figs. 4–6 show the variation damping ratio when the layer is located along the longitudinal direction but along a different circumferential strip of finite elements. Fig. 4 shows a relatively low damping ratio for all modes except for the first mode where as the layer position is shifted from the clamped end towards the middle, it increases to a maximum. All the modes show a low value of damping ratio when the layer is located at the middle. Modes 5 and 6 show a decreasing trend when the layer is shifted from the clamped end to the middle. Fig. 5 shows the damping ratio pattern when the layer is located at the third finite element longitudinal strip. From the figure it is

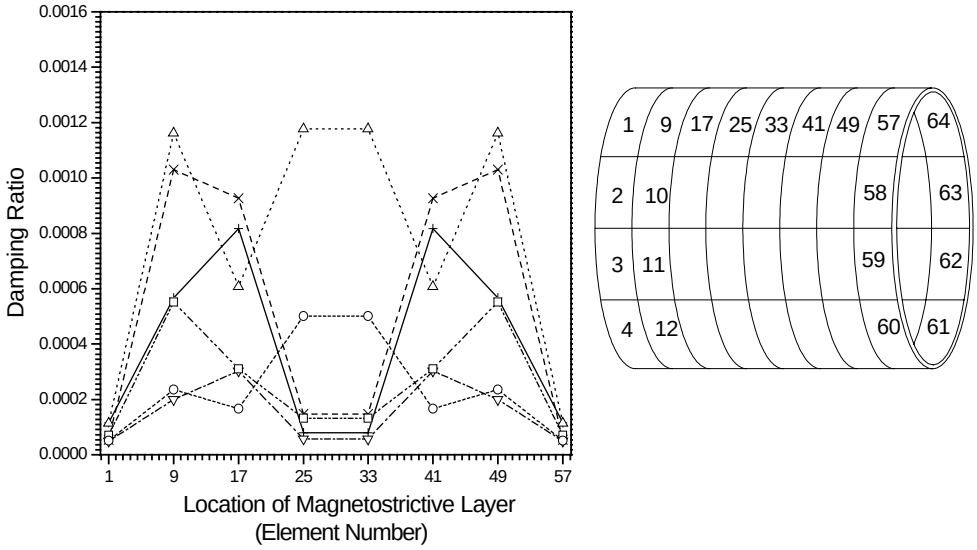

Fig. 3. Variation of damping ratio with respect to the location of magnetostrictive layer along the first longitudinal strip:–+–, mode 1; –×–, mode 2; ···Δ···, mode 3; –· ▽ ·–, mode 4; ··· □ ···, mode 5; ··· ○ ···, mode 6.

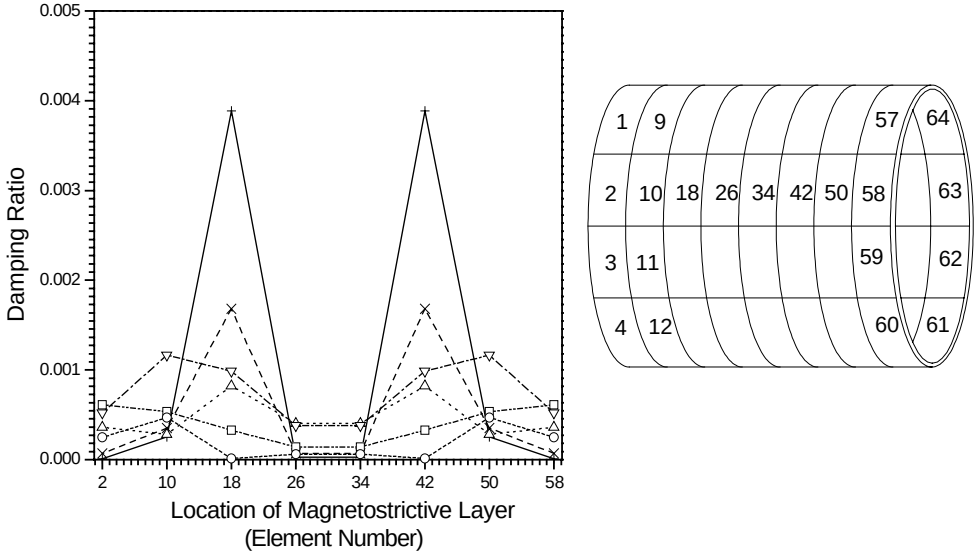

Fig. 4. Variation of damping ratio with respect to the location of magnetostrictive layer along the second longitudinal strip: –+–, mode 1; –×–, mode 2; ···Δ···, mode 3; –· ▽ ·–, mode 4; ··· □ ···, mode 5; ··· ○ ···, mode 6.

seen that for mode 1 the damping ratio increases from a lower value to a maximum and then drops to a minimum value as the location is shifted from the clamped end to the middle. Modes 3 and 4 show an increasing trend but as the layer is located near the middle, it attains a lower value. Modes 2 and 5 behave in an entirely opposite way till the layer reaches the middle. Mode 2 drops

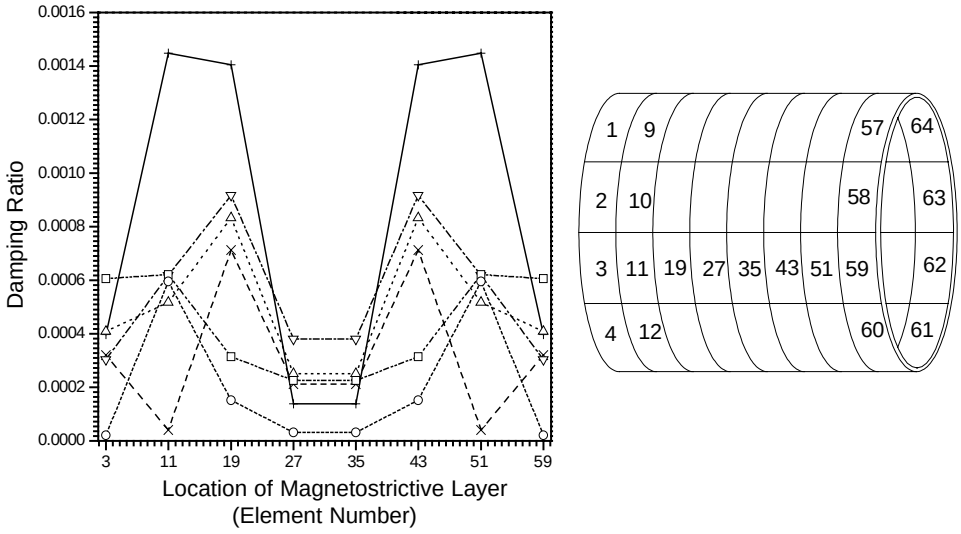

Fig. 5. Variation of damping ratio with respect to the location of magnetostrictive layer along the third longitudinal strip: –+–, mode 1; –×–, mode 2; ···Δ···, mode 3; –· ▽ ·–, mode 4; ··· □ ···, mode 5; ··· ○ ···, mode 6.

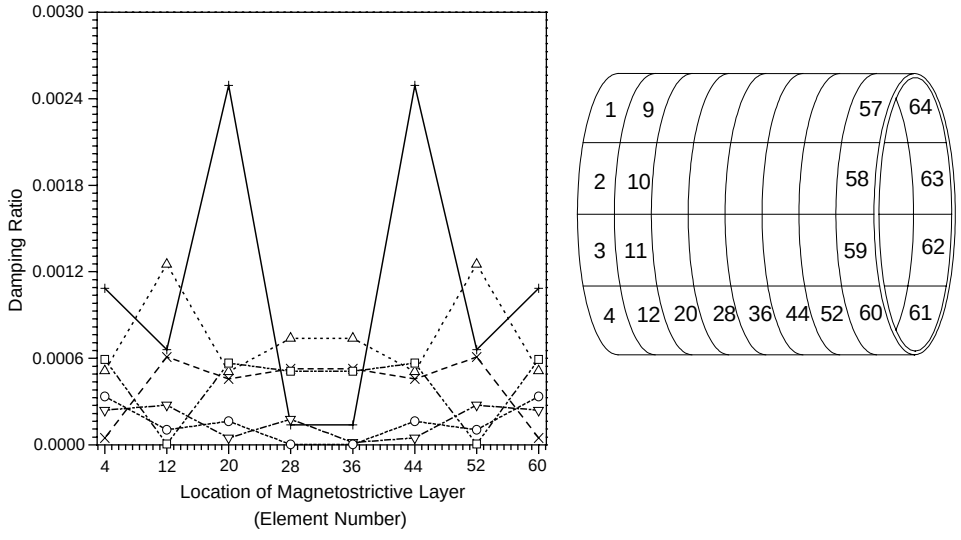

Fig. 6. Variation of damping ratio with respect to the location of magnetostrictive layer along the fourth longitudinal strip: –+–, mode 1; –×–, mode 2; ···Δ···, mode 3; –· ▽ ·–, mode 4; ··· □ ···, mode 5; ··· ○ ···, mode 6.

from the initial higher value and then increases and the decreases again near the middle, while mode 6 shows a decreasing trend from the clamped end to the middle of the shell. From Fig. 6 one can see that, except for modes 1 and 3 all other modes have a lower damping value as the layer is positioned along the bottom longitudinal strip of the shell. Mode 1 shows an alternating pattern in the damping ratio. It decreases from a high value when the layer is shifted from the clamped

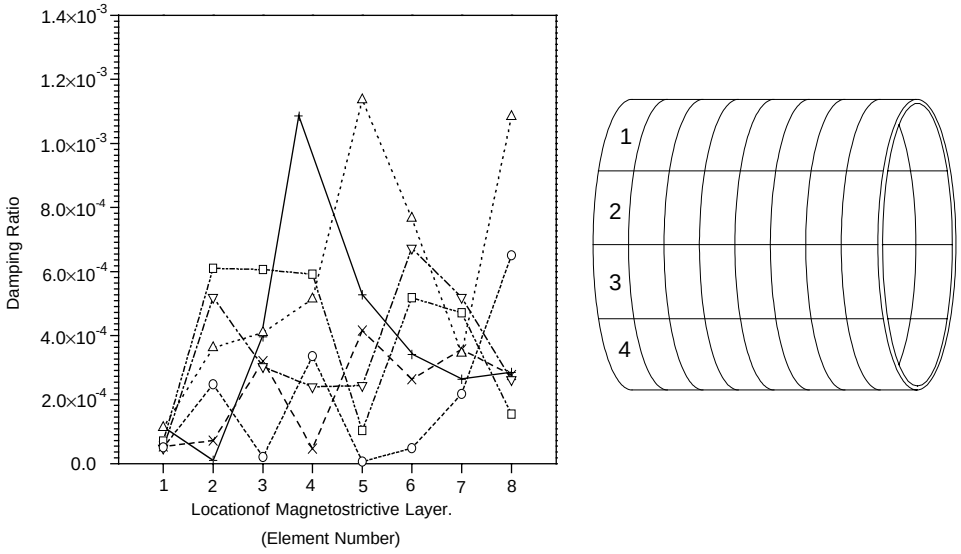

Fig. 7. Variation of damping ratio with respect to the location of magnetostrictive layer along the first circumferential strip: –+–, mode 1; –×–, mode 2; ···Δ···, mode 3; –· ▽ ·–, mode 4; ··· □ ···, mode 5; ··· ○ ···, mode 6.

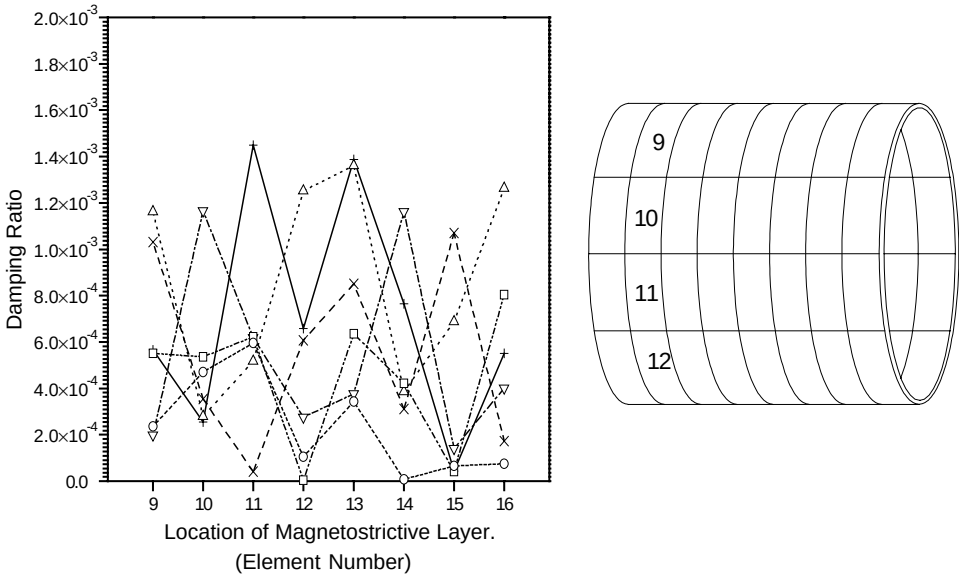

Fig. 8. Variation of damping ratio with respect to the location of magnetostrictive layer along the second circumferential strip: –+–, mode 1; –×–, mode 2; ···Δ···, mode 3; –· ▽ ·–, mode 4; ··· □ ···, mode 5; ··· ○ ···, mode 6.

end but increases to the highest value when shifted towards the middle. As the layer is positioned on either side of the middle, damping ratio attains a lowest value.

Figs. 7–10 show the variation of damping ratio as the magnetostrictive layer is located around the radial elements and shifted from the radial ring near the clamped end to the middle of the

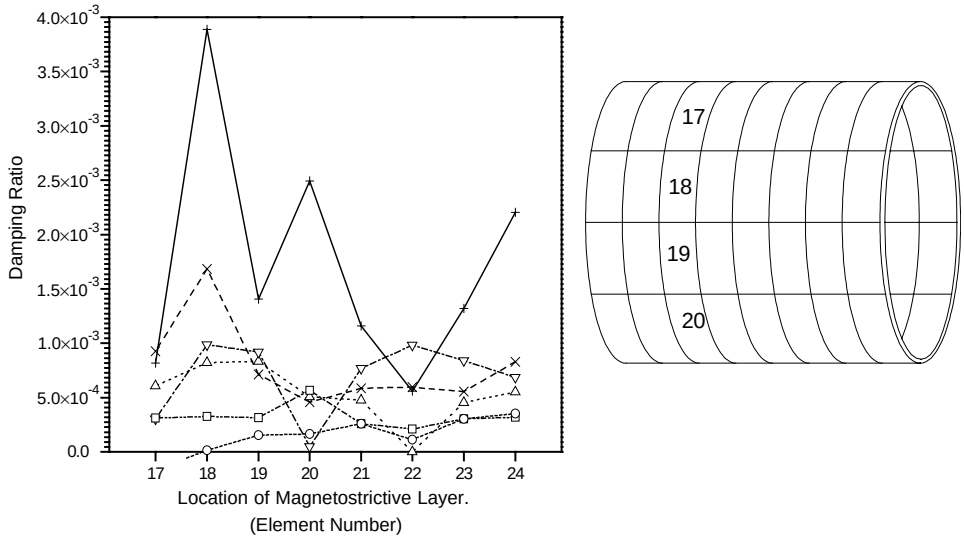

Fig. 9. Variation of damping ratio with respect to the location of magnetostrictive layer along the third circumferential strip: –+–, mode 1; –×–, mode 2; ···Δ···, mode 3; –· ▽ ·–, mode 4; ··· □ ···, mode 5; ··· ○ ···, mode 6.

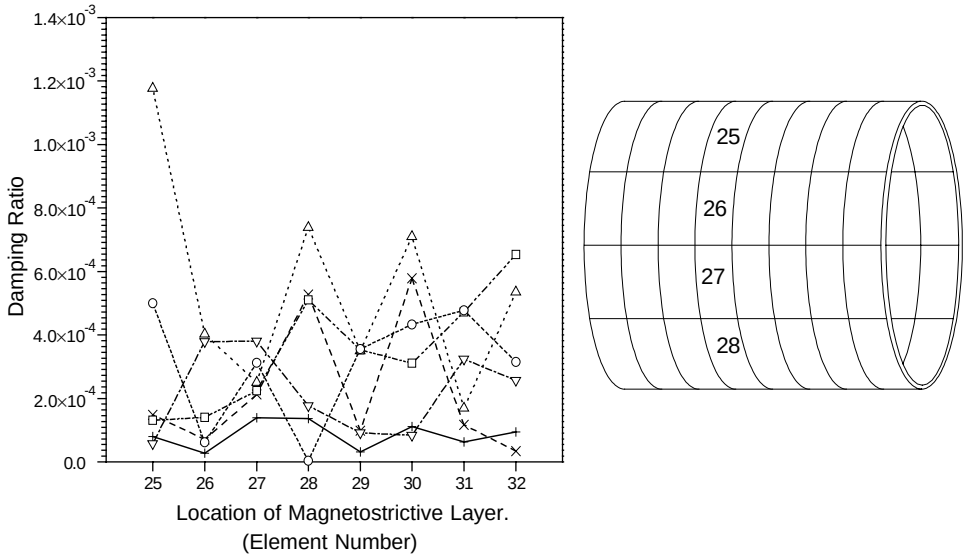

Fig. 10. Variation of damping ratio with respect to the location of magnetostrictive layer along the third circumferential strip: –+–, mode 1; –×–, mode 2; ···Δ···, mode 3; –· ▽ ·–, mode 4; ··· □ ···, mode 5; ··· ○ ···, mode 6.

shell. Fig. 7 indicates that the damping ratio alternates as the location is shifted along the radial directional elements for almost all modes. Modes 1 and 3 have a maximum damping value when the layer is positioned at the bottom of the shell. Fig. 8 also exhibits the same pattern as that of Fig. 7. As the location of the layer is moved from the clamped end towards the middle of the shell,

mode 1 alone has a significant damping value. All other modes have a minimum value when the layer is placed around the radial elements as shown in Fig. 9. Fig. 10 features the variation of damping ratio when the layer coil pair is located around the radial elements near the middle of the shell. Mode 1 has a minimum value of damping ratio. Mode 3 alone has a significant variation of damping ratio as it decreases from a maximum at the first element and alternatively varies as the position is changed around the radial elements.

5. Conclusions

In the present study, a finite element formulation is derived for shell with a magnetostrictive layer on top. The mathematical finite element model developed is consistent with the physics of the problem, unlike earlier formulations reported in the literature. A parametric study has been carried out for clamped–clamped boundary condition as well as for different location of actuating coils. This study seems to indicate that the location of the actuating coil to obtain better damping depends on the circumferential mode shapes. In general the maximum damping is obtained when the location of magnetostrictive layer is located at a point on the shell where the displacement is maximum for that mode.

References

[1] D.V. Wallerstein, M.O. Peach, Magnetoelastic buckling of beam and thin plates of magnetically soft material, Journal of Applied Mechanics 39 (1972) 451–455.
[2] K. Miya, T. Takagi, K. Someya, Experimental and theoretical study on magnetoelastic buckling of a ferromagnetic cantilever beam-plate, Journal of Applied Mechanics 45 (1978) 355–360.
[3] K. Miya, T. Takagi, Y. Ando, Finite-element analysis of magnetoelastic buckling of ferromagnetic beam plate, Journal of Applied Mechanics 47 (1980) 377–382.
[4] S.A. Ambartsumian, Magnetoelasticity of thin plates and shells, Applied Mechanics Reviews 35 (1) (1982) 1–5.
[5] M.J. Sablik, D.C. Jiles, Coupled magnetoelastic theory of magnetic and magnetostrictive hysteresis, IEEE Transactions on Magnetics 29 (1993) 2113–2123.
[6] J. Hudson, S.C. Busbridge, A.R. Piercy, Magnetomechanical coupling and elastic moduli of polymer-bonded terfenol composites, Journal of Applied Physics 83 (1998) 7255–7260.
[7] M.J. Dapino, R.C. Smith, A.B. Flatau, Structural-magnetic strain model for magnetostrictive transducers, IEEE Transactions on Magnetics 36 (2000) 545–556.
[8] Yoshio Yamamoto, Hiroshi Eda, Teruo Mori, Amer Rathore, Three dimensional magnetostrictive vibration sensor: development, analysis and application, Journal of Alloys and Compounds 258 (1997) 107–113.
[9] V. Krishnamurty, M. Anjanappa, Y.F. Wu, The use of magnetostrictive particle actuators for vibration attenuation of flexible beams, Journal of Sound and Vibration 206 (2) (1997) 133–149.
[10] J.N. Reddy, J.I. Barbosa, Vibration suppression of composite laminates with magnetostrictive layers, Proceedings of the International Conference on Smart Materials, Structures and Systems, Bangalore, India, July 7–10, 1999, pp. 377–384.
[11] O.C. Zienkiewicz, Finite Element Methods Used in Engineering Science, McGraw-Hill, London, 1979.
[12] J.D. Kraus, Electromagnetics, 3rd Edition, McGraw-Hill, New York, 1992.
[13] E. Anderson, Z. Bai, C. Bischof, S. Blackford, J. Demmel, J. Dongarra, J. Du Croz, A. Greenbaum, S. Hammarling, A. Mckenney, D. Sorensen, LAPACK User's Guide, 3rd Edition, SIAM, Philadelphia, 1999.